Journal of Molecular Liquids 309 (2020) 113209

Contents lists available at ScienceDirect

Journal of Molecular Liquids

journal homepage: www.elsevier.com/locate/molliq

Theoretical investigation of the adsorption behaviors of fluorouracil as an anticancer drug on pristine and B-, Al-, Ga-doped C36 nanotube

Mustafa Kurban [a], İskender Muz [b,*]

[a] Department of Electronics and Automation, Kırşehir Ahi Evran University, 40100 Kırşehir, Turkey
[b] Department of Mathematics and Science Education, Nevşehir Hacı Bektaş Veli University, 50300, Nevşehir, Turkey

ARTICLE INFO

Article history:
Received 28 February 2020
Received in revised form 23 March 2020
Accepted 21 April 2020
Available online 30 April 2020

Keywords:
Carbon nanotube
Fluorouracil
Doping
Adsorption
NCI-RDG analysis
DFT

ABSTRACT

Density functional theory (DFT) is used to examine the formation possibility of a stable interaction between 5-fluorouracil (5-FU) drug molecule and a pristine, boron (B), aluminum (Al), and gallium (Ga)-doped carbon nanotube (CNT). The structural, electronic, optical and reactivity properties of mentioned complexes are investigated in detail. Adsorption energies between the CNT and 5-FU are calculated in the range of −3.79 and −4.38 kcal/mol. Herein, the adsorption of the 5-FU on B-doped CNT is very weak, while stronger adsorption takes place in the case of Al- and Ga-doped CNTs. The results mean that the Al and Ga dopant increases the adsorption capacity of CNT with enhancing its interactions with oxygen atoms of the 5-FU. The charge transfer from adsorbed the 5-FU to Al- and Ga-doped CNTs was confirmed by the natural bond orbital, Mulliken charges, FBO and LBO analyses. It is found that the adsorption of 5-FU on Al-doped CNT is relatively stronger than that of Ga-doped CNT. The NCI-RDG analyses also verify these findings. The first absorption peaks suggest that the B-, A, Ga doped CNTs can absorb in the visible light region. Finally, Al-doped CNT has more desirable properties to use it as a drug delivery system.

1. Introduction

Targeted therapy for chronic diseases such as cancer has become the primary concern of researchers because of the limitations and serious side effects of anticancer drugs associated with existing treatments to the healthy cells [1,2]. Therefore, materials that can carry these drugs and deliver them specifically to cancers have attracted increasing attention because they are biocompatible and biodegradable, and they can encapsulate some drug molecules in their active sites. Among them, carbon nanotubes (CNTs), one-dimensional π-electron conjugation, as drug delivery tools have shown great promise for cancer treatment [3–6] due to their exceptional properties [7–11].

Anticancer drugs are not selective enough to have an impact only on cancer cells. For example, 5-Fluorouracil (5-FU) is an anticancer drug for its broad antitumor activity [12,13]. However, it includes cytotoxic anticancer agents that cause harmful side effects on both normal and cancer cells [14–18]. So, it is highly significant to reduce the toxic side effects in healthy cells induced by drugs and achieve an effective drug delivery to cancer cells. In this context, nanocarriers have been considered for the target-specific 5-FU drug delivery to the target site [19,20]. Moreover, the nanoparticles (NPs) [21], nanogels [22], chitosan NPs [23], cationic cyclodextrin/alginate chitosan nanoflowers [24], magnetic NPs [25] have been used as potential delivery tools for 5-FU delivery. When it comes to carbon-based materials, many attempts have been made to get a thoughtful insight into the interaction of carbon surfaces with different molecules [26,27]. Especially, functionalized carbon-based materials are nowadays a hot topic due to their excellent material properties [28–30]. For instance, the interactions of 5-FU drug with Al-doped C_{60} fullerene and graphene layers give rise to an improvement for drug delivery features of the materials [31,32]. On the other hand, Si-doped phagraphene is more suitable for adrucil delivery due to its desirable and harmless adsorption properties [33].

Determining the electronic and adsorption properties of the 5-FU drug on the surface of CNT is the key tool to understand bonding and reactivity features. Thus, in this study, we have carried out the adsorption of 5-FU drug molecule on the surface of B-, Al- and Ga-doped CNTs to figure out its structural, electronic, optical and reactivity properties and compare to the pristine CNT. B-, Al-, Ga-doped CNTs are more reactive and catalytic due to their extremely small size and large surface area. The reason why B, Al and Ga atoms are chosen as a dopant is that they have the lowest binding energy among the CNT models studied compared to other atoms (Si, Ge, N, P and As) [9]. In the periodic table, IIIA group (B, Al and Ga) atoms are located to the left of C atom and have a lower electronegativity. Thus, these dopant atoms will cause an electron-deficient site in the structure of CNTs. Also, we chose C36 CNT, because it has approximately a diameter of 4 Å, which is the narrowest attainable that can remain energetically stable, as

* Corresponding author.
E-mail address: iskendermuz@yahoo.com (İ. Muz).

https://doi.org/10.1016/j.molliq.2020.113209
0167-7322/

reported in previous studies [9,34]. In this context, the interaction of a 5-FU drug molecule with the surface of C36, C35B, C35Al and C35Ga CNTs have been performed using DFT methods based on Mulliken charges, Fuzzy and Laplacian bond orders as well as NCI-RDG analyses. The absorption properties based on time-dependent (TD)-DFT also analyzed. To the best of our knowledge, there is no experimental application on B-, Al- and Ga-doped CNTs. Thus, the potential applications of them have not been expanded to the clinical trial stage as yet. Hopefully, our results will predict the next clinical and experimental studies.

2. Computational details

Density functional theory (DFT) has been used to examine the formation possibility of a stable interaction between fluorouracil (5-FU) drug molecule and pristine (C36), boron (B), aluminum (Al), and gallium (Ga)-doped $3 \times 3 \times 3$ carbon nanotubes (CNTs). Before the geometry optimization process, individual B, Al and Ga from the central region of the CNT (C36) are substituted with one of its C atoms. Besides, both ends of the C36 and doped (C35B, C35Al and C35Ga) CNTs are also capped with hydrogen atoms to minimize the edge effects. All the optimized geometries and vibrational frequencies were carried out using Gaussian 09 software [35] at the level of DFT in combination with the B3LYP/6-31G(d) [36]. At that viewpoint, it is important to note that dispersion effects have been also used for molecular adsorption on carbon nanotubes in previous experiment studies [37,38]. Despite of insufficient description of dispersion in B3LYP, it is the popular functional used in the CNTs [39–42] and it produces suitable results with less computational time.

The adsorption energy (E_{ad}) between 5-FU drug molecule and CNTs is computed using the following formula:

$$E_{ad} = E\left(\frac{CNTs}{FU}\right) - E(CNTs) + E(FU) + E(BSSE) \quad (1)$$

where $E(CNTs/5\text{-}FU)$ is the total energies of the adsorbed fluorouracil on the pristine and doped CNT. $E(CNTs)$ and $E(5\text{-}FU)$ are the total energies of pristine/doped CNTs and 5-FU drug molecule, respectively. $E(BSSE)$ is defined as the basis set superposition error (BSSE), which is calculated by the counterpoise method to determine highly accurate adsorption energy [43].

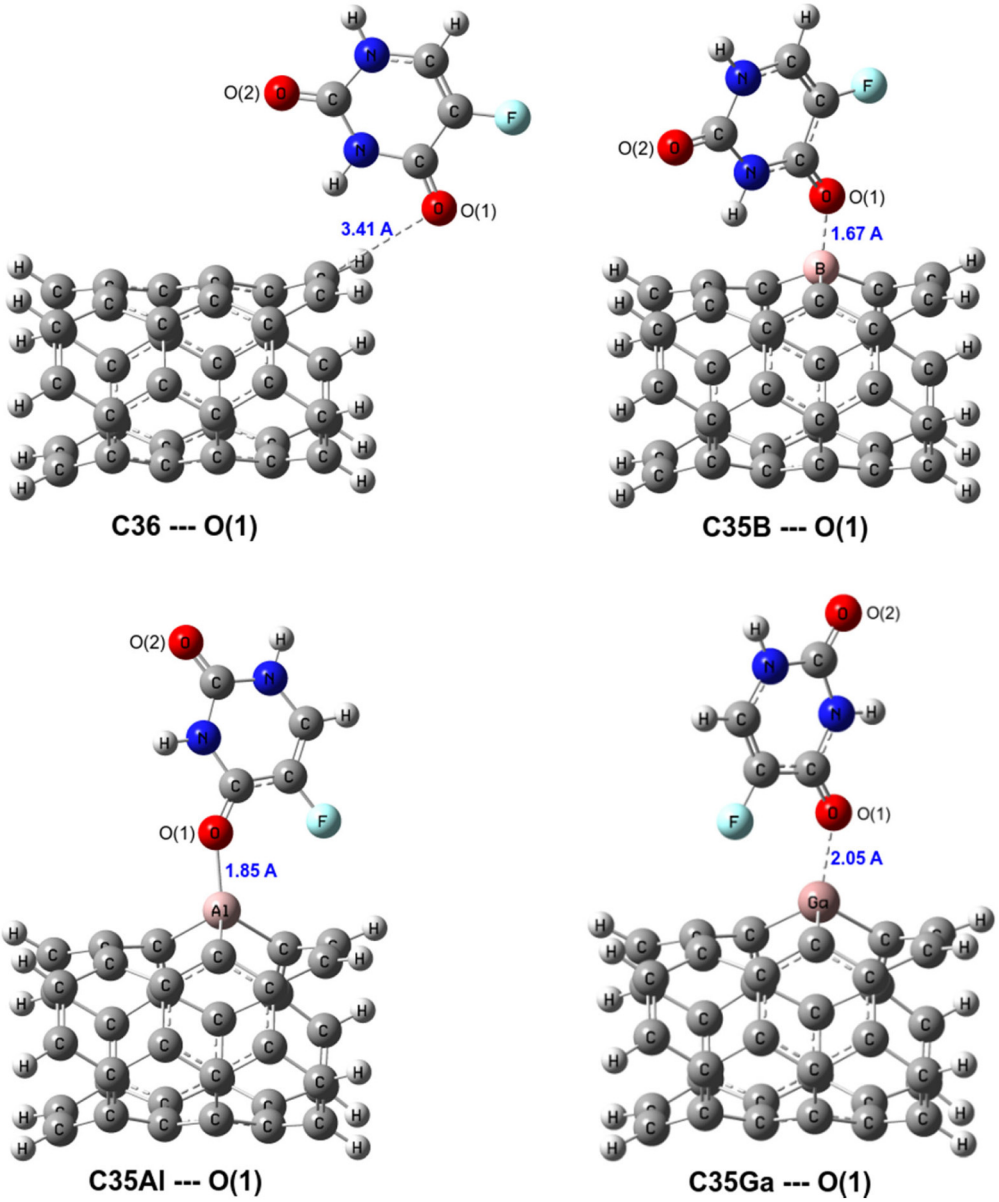

Fig. 1. Relaxed structures of O(1) configuration for adsorption states of 5-FU drug molecule onto the pristine, B-, Al- and Ga-doped CNTs.

The vertical ionization potential (*VIP*) and vertical electron affinity (*VEA*) are calculated as follows: [$VIP = E^{cation} - E^{neutral}$] and [$VEA = E^{neutral} - E^{anion}$]. In these equations, the *VIP* is the energy difference between the ground state of the cation (E^{+}) and the ground state of the neutral (E^{0}) at the geometry of the neutral. *VEA* is defined as the energy difference between the ground state of the neutral (E^{0}) and the ground state of the anion (E^{-}) at the geometry of the neutral. For 5-FU drug molecule adsorbed on the pristine and doped CNTs, the global reactivity descriptors [44–46] such as chemical hardness (η), chemical potential (μ) and electrophilicity index (ω) and maximum amount of electronic charge index (ΔN_{tot}) are calculated. GaussSum 3.0 program is applied to draw density of state diagrams [47]. The non-covalent interactions (NCI), Fuzzy bond orders (FBO) and Laplacian bond orders (LBO) are performed using the Multiwfn program [48]. Besides, molecular structures and graphs drawing the isosurfaces are also visualized by GaussView [49] the visual molecular dynamics (VMD) software [50], respectively. In addition, TD-DFT with CAM-B3LYP functional [51] and 6-31G(d) basis set is performed for estimating UV–visible (UV–vis) absorption spectra because B3LYP underestimates excited state energies [52,53].

3. Results and discussions

The structural and stability features of pristine and B-, Al- and Ga-doped CNTs have been reported in previous studies [9,10]. In this study, we have calculated the various configurations for the 5-FU adsorbed on the surface of pristine and doped (C35X; X = B, Al and Ga) CNTs based on O(1) (O atom adjacent to the F atom), O(2) (O atom between N atoms), F (F atom) interaction points. Our calculations show that doped CNTs prefer to interact with the O(1) and O(2) points of the 5-FU. These results are in agreement with different absorbent in

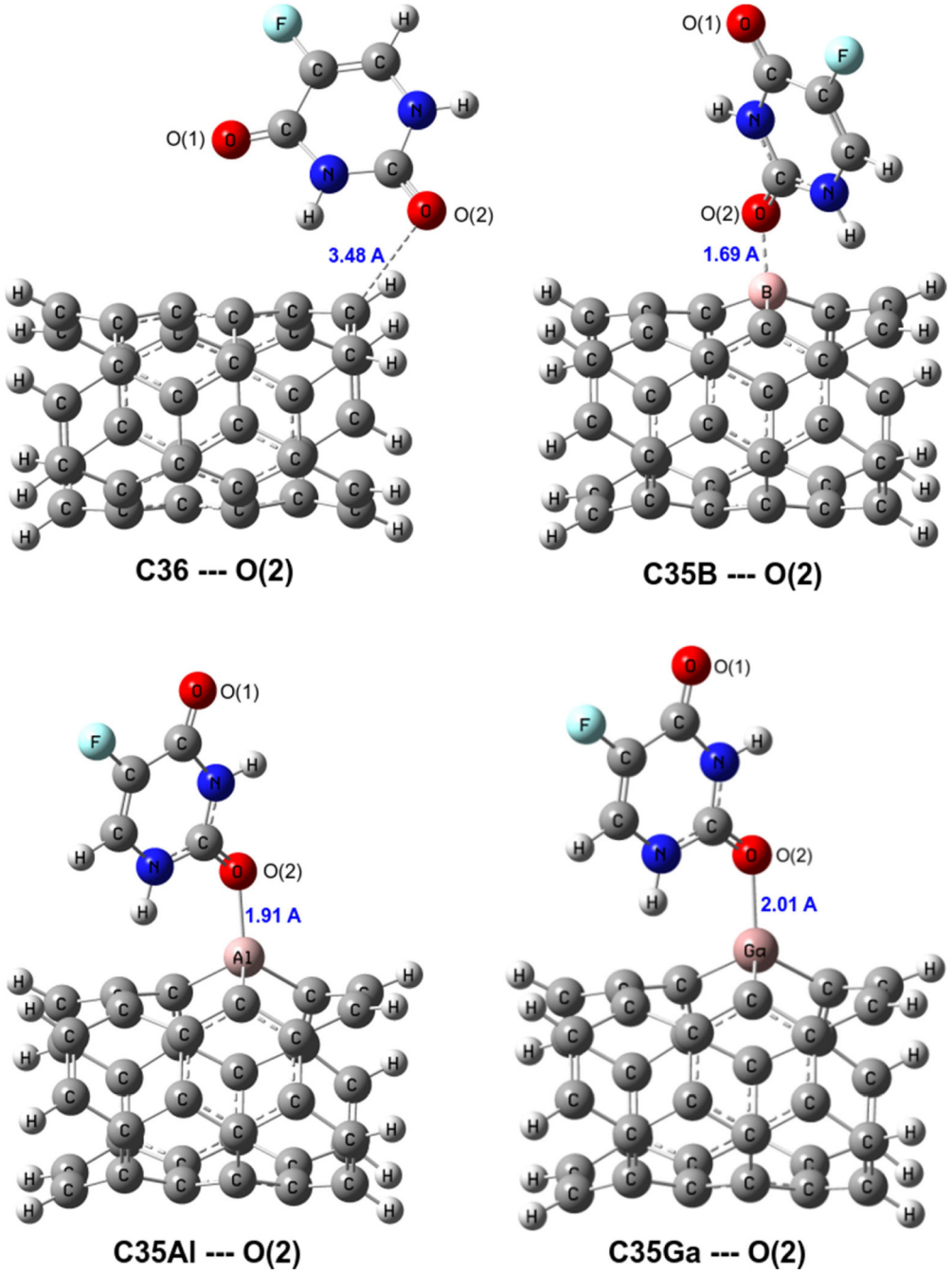

Fig. 2. Relaxed structures of O(2) configuration for adsorption states of 5-FU drug molecule onto the pristine, B-, Al- and Ga-doped CNTs.

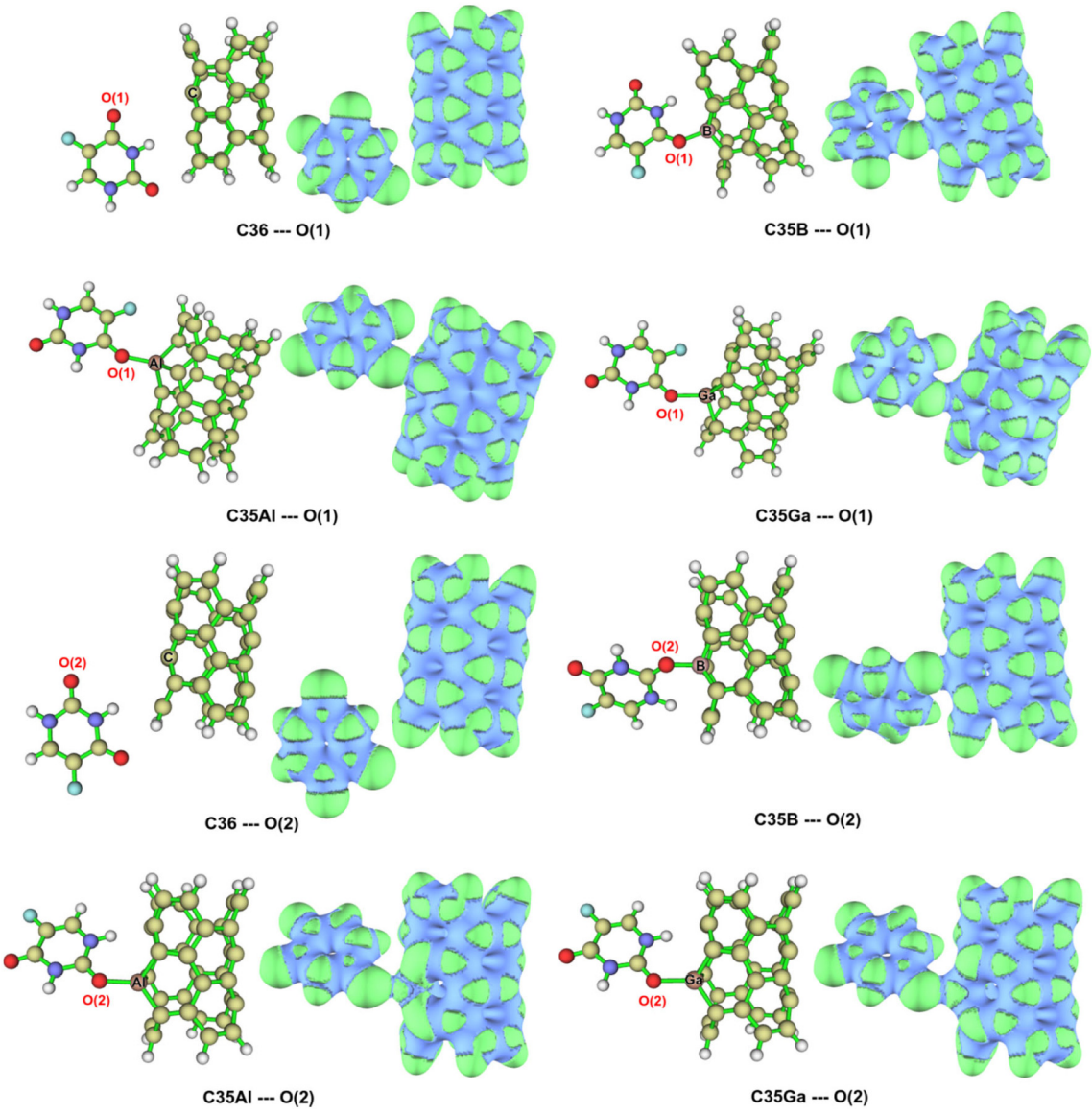

Fig. 3. Molecular electrostatic surface potential (MESP) of the pristine CNT + 5-FU complexes, 5-FU adsorbed on the surface of B-, Al- and Ga-doped CNTs.

the literature [31,54,55]. The obtained two stable configurations between the studied CNTs and 5-FU drug molecule are investigated in detail. The bond lengths of relaxed structures in terms of O(1) and O(2) configurations are presented in Figs. 1-2.

One can see that the relaxed C — O(1) and C — O(2) bond lengths in O(1) and O(2) configurations are approximately 3.41 Å and 3.48 Å, respectively. Because of the interaction range, the CNT and 5-FU do not interact with each literature [31]. Based on the results, C35B — O(1)/O(2), C35Al — O(1)/O(2) and C35Ga — O(1)/O(2) bond lengths are found to be 1.67/1.69 Å, 1.85/1.91 Å and 2.05/2.01 Å, respectively (see Figs. 1-2). This means that the CNT and 5-FU are in the interaction range. From molecular electrostatic surface potential (MESP), the 5-FU can be considered as the possible active site for interaction with the doped CNTs (see Fig. 3). We also note that Al- and Ga-doped CNTs prefer to interact with the oxygen atoms of the 5-FU.

The adsorption energies (E_{ad}) of interactions between pristine/doped CNTs and 5-FU considering O(1) and O(2) configurations are listed in Table 1. The E_{ad} of pristine CNT and 5-FU molecule are

Table 1
Electronic and reactivity properties of pristine CNT + 5-FU complexes, 5-FU adsorbed on the surface of B-, Al- and Ga-doped CNTs. O(1) and O(2) according to Figs. 1-2.

Complex	E_{ad} (kcal/mol)	HOMO (eV)	LUMO (eV)	E_g (eV)	VIP (eV)	VEA (eV)	η (eV)	ω (eV)	ΔN_{tot} (eV)
C36 --- O(1)	−3.79	−4.53	−1.79	2.74	5.90	0.54	1.37	3.64	2.31
C36 --- O(2)	−4.38	−4.52	−1.77	2.75	5.89	0.52	1.38	3.60	2.29
C35B --- O(1)	−6.30	−3.65	−2.34	1.31	4.91	1.01	0.66	6.85	4.57
C35B --- O(2)	−7.10	−3.75	−2.2	1.55	5.01	1.00	0.78	5.71	3.84
C35Al --- O(1)	−30.15	−3.46	−2.25	1.21	4.63	1.11	0.61	6.74	4.72
C35Al --- O(2)	−36.00	−3.87	−2.35	1.52	5.11	1.18	0.76	6.36	4.09
C35Ga --- O(1)	−23.75	−3.50	−2.78	0.72	4.73	0.97	0.36	13.69	8.72
C35Ga --- O(2)	−30.10	−3.96	−2.42	1.54	5.20	1.24	0.77	6.61	4.14

calculated in the range of −3.79 and −4.38 kcal/mol, respectively, in good agreement with previous studies [31]. After one of C atoms on CNT was replaced by the dopant atom as B, Al, and Ga, the E_{ad} lie in the range around −6.30 and −36.00 kcal/mol (see Table 1) which corresponds very weak the adsorption between B-doped CNTs and 5-FU. On the other hand, the stronger adsorption takes place in the case of 5-FU adsorbed on the surface of Al- and Ga-doped CNTs. The E_{ad} of 5-FU on the Al-doped CNTs are relatively greater than that of Ga-doped CNTs. Besides, O(2) interaction points are more favorable than O(1). Herein, the obtained results reveal that Al- and Ga-doped CNTs can be used as possible delivery tools for the 5-FU drug. At that viewpoint, in this study, we have demonstrated that dopant atoms, especially Al, help increase the adsorption onto the delivery CNTs of 5-FU drug. This could lead to more effective and convenient cancer treatments with fewer side effects. Here, it is possible the side effects of these dopants due to their toxicity to healthy cells. On the other hand, considering successful drug delivery properties of these dopants and the harmful side effects of the 5-FU drug, the toxicity effects of the dopants may be a further need to investigate the ability of them to induce toxic damage.

The other important physical parameters, the highest occupied molecular orbital (HOMO) and the lowest unoccupied molecular orbital (LUMO) levels, and their difference the energy gap (E_g) have been carried out to better understanding the stability of the system. The results are tabulated in Table 1. Besides, the *VIP*, *VEA*, η, μ, ω, and ΔN_{tot} values for 5-FU interacting with pristine and doped CNTs are given in Table 1. The E_g values of C36 — O(1) and C36 — O(2) complexes are found to be 2.7 eV. Moreover, the E_g values are significantly reduced in absorptions O(1) and O(2) after doping B, Al and Ga atoms, which is in excellent agreement with similar studies [56,57]. Fig. 4 shows the density of states (DOS) of pristine and doped CNT + 5-FU complexes, which are calculated in the energy range of −10 to 0 eV. From DOS analysis, B-, Al-, Ga-doped CNTs give rise to a decrease in the E_g, thus significantly decrease the conductivity. This trend is mainly due to the formation of new energy levels between the HOMO and LUMO levels of pristine CNT + 5-FU complex.

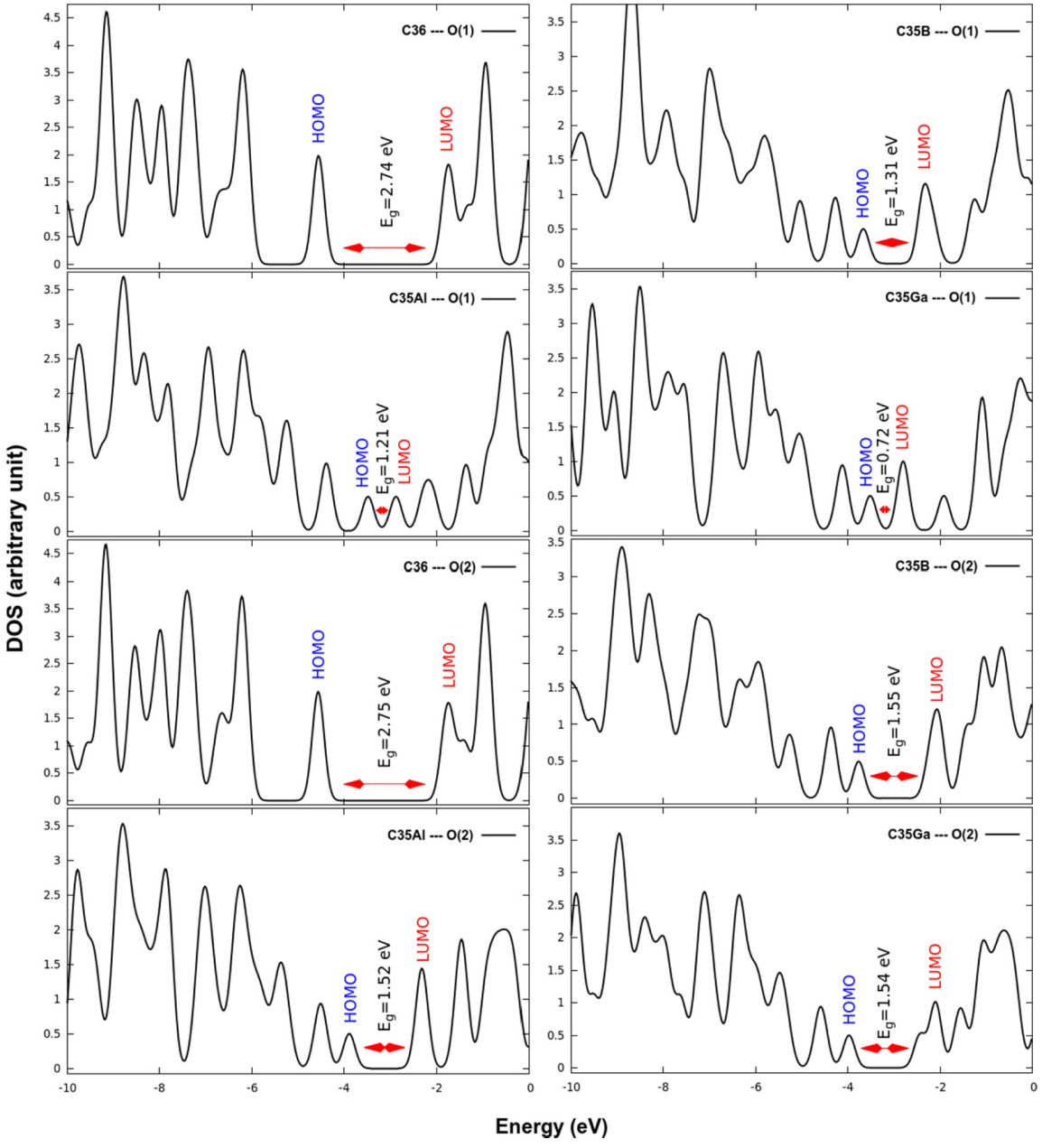

Fig. 4. DOS of pristine CNT + 5-FU complexes and 5-FU adsorbed on the surface of B-, Al- and Ga-doped CNTs. O(1) and O(2) according to Figs. 1-2.

When it comes to B-, Al- and Ga-doped CNTs, a decrease in η and *VIP* is noted (Table 1). The η of 5-FU on the B-doped CNTs is also found to be larger than the Al- and Ga-doped CNT which means that the 5-FU on the Al- and Ga-doped CNT shows more resistance to charge transfer compared to the B-doped CNT. On the other hand, the changes in the E_g values for the mentioned molecular systems are compatible with the trend of the η and *VIP* (see Table 1). On the other hand, an increase in the *VIP* is observed for the 5-FU on B-, Al- and Ga-doped CNT when compared to pristine CNT + 5-FU complex, whereas an increase in *VEA*, ω, ΔN_{tot} are also predicted (Table 1). This means that the 5-FU on B-, Al- and Ga-doped CNT has a higher tendency to accept electron than that of the pristine CNT complex. This fact suggests that 5-FU drug on the surface of B-, Al- and Ga-doped CNTs interacts more efficiently.

The donor-acceptor interactions can be predicted using NBO results [58]. Thus, the bonding properties of pristine and doped CNT + 5-FU complexes are investigated based on Natural Bond Orbital (NBO) and bond order (FBO and LBO) calculations. The NBO and Mulliken charges propose the presence of donor-acceptor interactions between B/Al/Ga and O atoms of the 5-FU on the doped CNT. Also, FBO [59] and LBO [60] can be traditionally used to assess how strong covalent bonding occurs between two atoms [61]. The calculated FBO and LBO values are also given in Table 2. The FBO and LBO values for 5-FU adsorbed on the surface of B-, Al- and Ga-doped CNTs are listed in Table 2. FBO and LBO analyses suggest the formation of 5-FU adsorbed on the surface of Al- and Ga-doped CNTs since Al — O(1), Al — O(2), Ga — O(1) and Ga — O(2) bonds predicted to have high value. However, the FBO values of 5-FU adsorbed on the surface of B-doped CNT are lower than that of 5-FU adsorbed on the surface of Al- and Ga-doped CNTs, and there are no LBO values. The FBO and LBO values have also a strong correlation with the bond lengths. Al — O(2) and Ga — O(1) bonds are slightly weaker than Al — O(2) and Ga — O(1) bonds, respectively, since their bond lengths are longer (see Figs. 1-2), but they have a smaller FBO and LBO values (see Table 2). NBO, FBO and LBO analyses indicate a possible bonding interaction between the dopants in CNTs and the oxygen atoms of the 5-FU drug molecule. It is also worth to note that these analyses indicate the possible donor-acceptor relations between the Al- and Ga-doped CNTs and 5-FU drug molecule.

Ultraviolet–visible (UV–vis) absorption spectra are some of the most fundamental optical properties of all complexes. UV–vis absorption spectra for pristine/doped CNTs +5-FU complexes are calculated by using TD-DFT and plotted in Fig. 5. The maximum UV–vis absorption spectrum values of pristine CNTs +5-FU complexes indicate an absorption peak located in the range of 399.4 and 401.6 nm in the visible light region. The absorption spectrum of 5-FU adsorbed on the surface of B-doped, Al-doped and Ga-doped CNTs are also observed at wavelengths of 401–484 nm, 501–564 nm and 597–611 nm, respectively (see Fig. 5). We note that the presence of a B, Al and Ga doping increases significantly absorption in the visible light region.

Figs. 6-7 show the scatter plots of reduced density gradient (RDG) vs. sign($\lambda 2$)ρ and non-covalent interaction (NCI) isosurfaces for studied complexes. These plots can be an important tool to understand the attraction and repulsion of interactions as well as to evaluate and characterize the nature of the weak or strong interactions [62]. The larger negative values of sign($\lambda 2$) point out stronger attractive interaction about charge density (ρ) = −0.04 (such as H-bonds and dipole-dipole interactions), whereas positive values make a sign the strong repulsion interaction (steric) about $\rho = 0.04$. Besides, $\rho = 0$ also corresponds to the Van der Waals (vdW) forces [62]. In plots of NCI isosurfaces, green regions represent vdW interactions, however blue regions are strong interactions, and red regions indicate a strong steric effect. It can be seen from Figs. 6a-7a that there are Van der Waals (vdW) forces about $\rho = 0$ in pristine CNTs +5-FU (C36 — O(1) and (C36 — O(2)) complexes. Similarly, the effect of vdW forces can be observed clearly in C35B — O(1) and C35B — O(2). For 5-FU adsorbed on the surface of Al- and Ga-doped CNTs, the number of RDG points (around 0.6 in the y-axis) shows an increase in strong attractive interaction regions (see Figs. 6c-6d and 7c-7d). For C35Al — O(1) and C35Al — O(2) complexes, it can be seen that there are evident deep spikes in a range of −0.03 and − 0.04 (indicated by blue ellipsoid), which indicate strong attractive interaction (see Figs. 6c-7c). Besides, there is almost no

Table 2
Population analyses of pristine CNT + 5-FU complexes, 5-FU adsorbed on the surface of B-, Al- and Ga-doped CNTs. O(1) and O(2) according to Figs. 1-2.

Complex	Atom	Valance number	Mulliken charge	NBO charge	FBO	LBO
FU	O [1]	6.548	−0.477	−0.568	–	–
	O [2]	6.597	−0.493	−0.616	–	–
C36	C	3.991	0.001	−0.004	–	–
C36 --- O(1)	C	4.026	−0.004	−0.042	–	–
	O [1]	6.541	−0.471	−0.561		
C36 --- O(2)	C	3.991	0.001	−0.005	–	–
	O [2]	6.593	−0.513	−0.612		
C35B	B	1.122	0.096	0.686	–	–
C35B --- O(1)	B	1.165	0.177	0.646	0.661	–
	O [1]	3.260	−0.235	−0.525		
C35B --- O(2)	B	1.161	0.179	0.655	0.644	–
	O [2]	3.275	−0.247	−0.572		
C35Al	Al	0.635	0.246	1.653	–	–
C35Al --- O (1)	Al	0.616	0.269	1.736	0.940	0.120
	O [1]	3.364	−0.281	−0.760		
C35Al --- O (2)	Al	0.627	0.240	1.718	0.850	0.098
	O [2]	3.360	−0.283	−0.735		
C35Ga	Ga	0.768	0.140	1.388	–	–
C35Ga --- O (1)	Ga	0.765	0.111	1.472	0.786	0.087
	O [1]	3.283	−0.259	−0.619		
C35Ga --- O (2)	Ga	0.736	0.106	1.470	0.847	0.095
	O [2]	3.332	−0.278	−0.673		

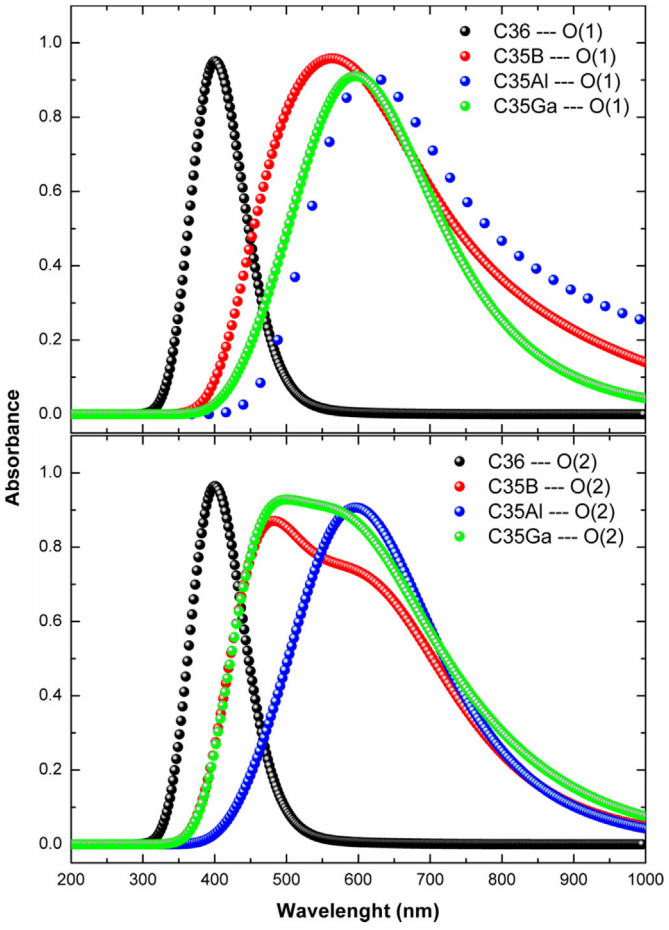

Fig. 5. UV–vis spectra of the pristine CNT + 5-FU complexes and 5-FU adsorbed on the surface of B-, Al- and Ga-doped CNTs. O(1) and O(2) according to Figs. 1-2.

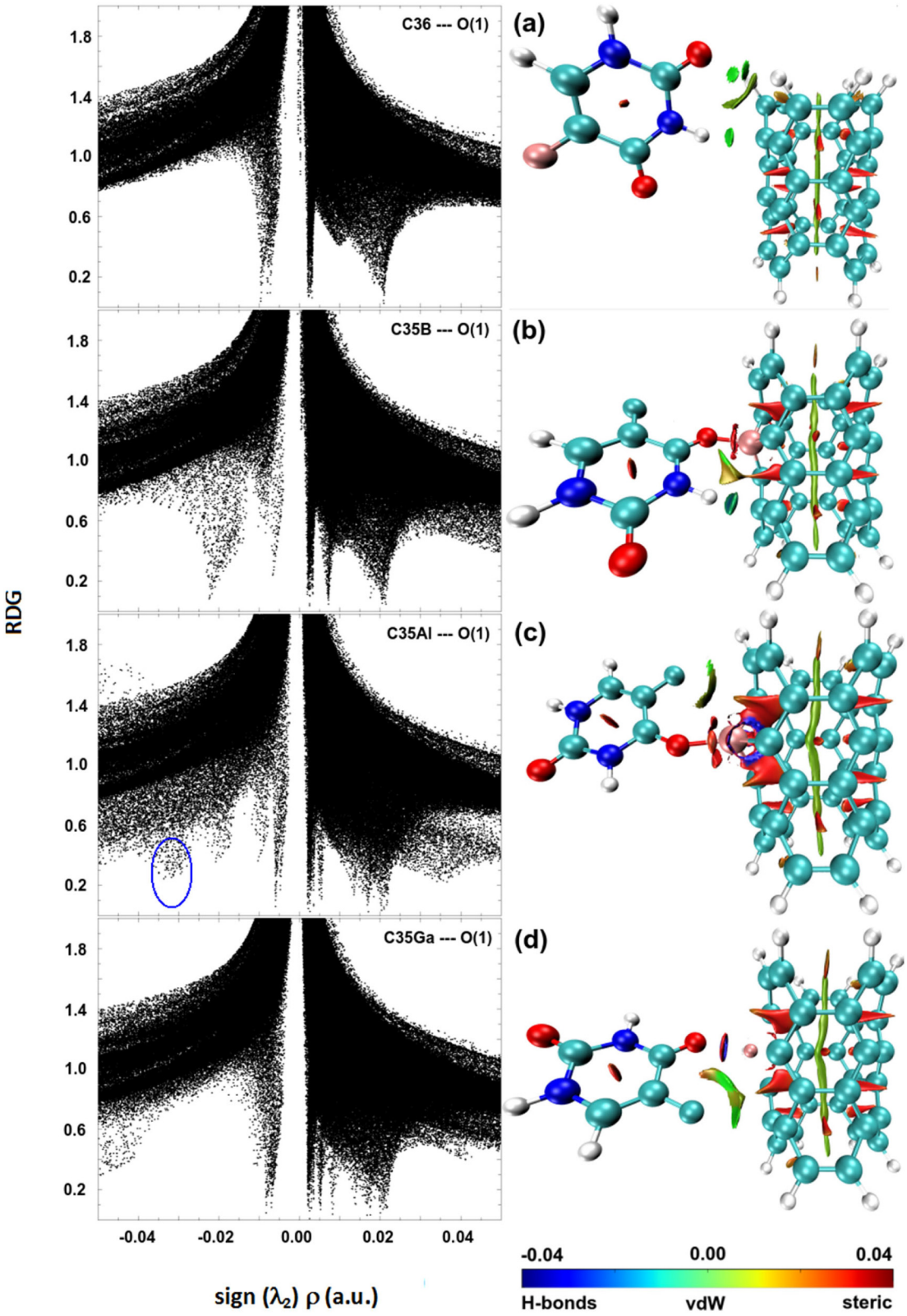

Fig. 6. The reduced density gradient (RDG) scatter plots (Left) and non-covalent interaction (NCI) isosurfaces (Right) of **(a)** C36 — O(1), **(b)** C35B — O(1), **(c)** C35Al — O(1) and **(d)** C35Ga — O(1). B/Al/Ga, C, H, O, and N atoms are shown in pink, light blue, white, red, dark blue, respectively.

obvious spike near zero (in $\rho = 0$) fields of the x-axis which verifies the presence of attractive interactions in C35Al — O(1) and C35Al — O (2) complexes. For C35Ga — O(2) complex, it can be seen an evident deep spike around −0.02 a.u. (see Fig. 7d). Although the number of RDG points increases in strong interaction region (around $\rho = -0.05$) for the C35Ga — O(1) complex (see Fig. 6d), there is no observed a deep spike in the attractive interaction region. For C35Ga — O(2) complex, there is no obvious spike as C35GaFig. 6dO

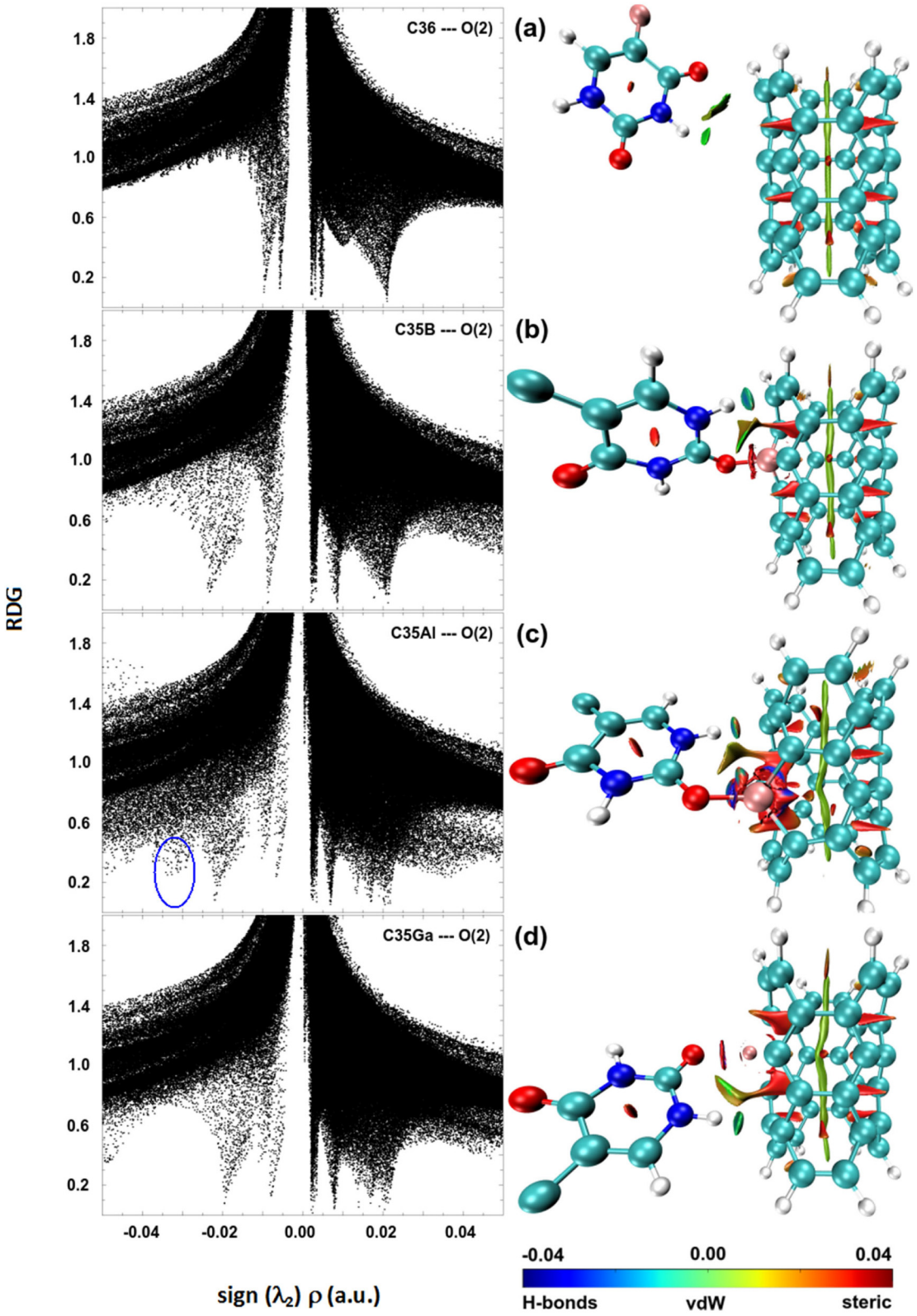

Fig. 7. The reduced density gradient (RDG) scatter plots (Left) and non-covalent interaction (NCI) isosurfaces (Right) of **(a)** C36 – O(2), **(b)** C35B – O(2), **(c)** C35Al – O(2) and **(d)** C35Ga – O(2). B/Al/Ga, C, H, O, and N atoms are shown in pink, light blue, white, red, dark blue, respectively.

(1) complex around $\rho = 0$ (see Fig. 6d). NCI-RDG analyses indicate that interactions between the 5-FU and the surface of Al-doped CNTs are stronger than that of Ga-doped CNTs, which is compatible with the E_{ad} values. It is worth to note that Al doping is the main source of strong attractive interaction when compared with the B- and Ga-doped CNT + 5-FU complexes.

4. Conclusions

In this study, some important structural, electronic, optical and reactivity properties of 5-FU drug molecule adsorbed on the surface of pristine, B-, Al-, and Ga-doped CNTs were investigated by DFT calculations. The adsorption energies between the Al- and Ga-doped CNTs and 5-FU are in the range of −30.15/−36.00 and −23.75/−30.10 kcal/mol. The charge transfer from adsorbed 5-FU molecule to Al- and Ga-doped CNTs is confirmed by the NBO, Mulliken charge, FBO and LBO, whereas there is very weak interaction between B-doped CNTs and 5-FU drug molecule. It is worth to note that FBO and LBO analyses have a strong correlation with the bond lengths. Also, the 5-FU drug molecule acts as an electron donor whereas the doped CNTs are electron acceptors. According to our results, Al and Ga dopants induces an increase in the adsorption capacity of CNT, thus improving its interactions with oxygen atoms of the 5-FU drug. However, NCI-RDG analysis shows that interactions between the 5-FU and the surface of Ga-doped CNT are weaker than that of Al-doped CNT, which is compatible with the formation energy. Also, the first absorption peaks from UV–vis spectra show all complexes can absorb in range of 399.4 and 596.8 nm in the visible light region. Overall, our results suggest the Al-doped CNT can be used as a delivery tool for cancer treatment.

CRediT authorship contribution statement

Mustafa Kurban: Supervision, Investigation, Conceptualization, Writing - original draft, Writing - review & editing, Data curation, Validation, Software. **İskender Muz:** Investigation, Methodology, Visualization, Writing - original draft, Writing - review & editing, Data curation, Software.

Acknowledgments

The numerical calculations reported were partially performed at TUBITAK ULAKBIM, High Performance and Grid Computing Centre (TRUBA resources), Turkey.

Declaration of competing interest

The authors declare that they have no known competing financial interests or personal relationships that could have appeared to influence the work reported in this paper.

References

[1] A. Albini, G. Pennesi, F. Donatelli, R. Cammarota, S. De Flora, D.M. Noonan, Cardiotoxicity of anticancer drugs: the need for cardio-oncology and cardio-oncological prevention, JNCI J. Natl. Cancer Inst. 102 (2010) 14–25, https://doi.org/10.1093/jnci/djp440.
[2] E. Chatelut, J.P. Delord, P. Canal, Toxicity patterns of cytotoxic drugs, Investig. New Drugs 21 (2003) 141–148, https://doi.org/10.1023/A:1023565227808.
[3] H. He, L.A. Pham-Huy, P. Dramou, D. Xiao, P. Zuo, C. Pham-Huy, Carbon nanotubes: applications in pharmacy and medicine, Biomed. Res. Int. (2013)https://doi.org/10.1155/2013/578290.
[4] N.G. Sahoo, H. Bao, Y. Pan, M. Pal, M. Kakran, H.K.F. Cheng, L. Li, L.P. Tan, Functionalized carbon nanomaterials as nanocarriers for loading and delivery of a poorly water-soluble anticancer drug: a comparative study, Chem. Commun. 47 (2011) 5235–5237, https://doi.org/10.1039/c1cc00075f.
[5] S.Y. Madani, N. Naderi, O. Dissanayake, A. Tan, A.M. Seifalian, A new era of cancer treatment: carbon nanotubes as drug delivery tools, Int. J. Nanomedicine 6 (2011) 2963–2979, https://doi.org/10.2147/IJN.S16923.
[6] A. Sanginario, B. Miccoli, D. Demarchi, Carbon nanotubes as an effective opportunity for cancer diagnosis and treatment, Biosensors-Basel 7 (2017)https://doi.org/10.3390/bios7010009.
[7] S.S. Begum, N.K. Gour, U. Sonavane, S.K. Ray, R.C. Deka, Computational studies of anti-cancer drug mediated by graphene and reaction mechanism of drug generated alkyl radical with guanine, J. Mol. Struct. 1196 (2019) 527–535, https://doi.org/10.1016/j.molstruc.2019.06.101.
[8] J.W.G. Wildoer, L.C. Venema, A.G. Rinzler, R.E. Smalley, C. Dekker, Electronic structure of atomically resolved carbon nanotubes, Nature 391 (1998) 59–62, https://doi.org/10.1038/34139.
[9] I. Muz, M. Kurban, A comprehensive study on electronic structure and optical properties of carbon nanotubes with doped B, Al, Ga, Si, Ge, N, P and As and different diameters, J. Alloys Compd. 802 (2019) 25–35, https://doi.org/10.1016/j.jallcom.2019.06.210.
[10] M. Kurban, Electronic structure, optical and structural properties of Si, Ni, B and N-doped a carbon nanotube: DFT study, Optik (Stuttg) 172 (2018) 295–301, https://doi.org/10.1016/j.ijleo.2018.07.028.
[11] E.-K. Lim, T. Kim, S. Paik, S. Haam, Y.-M. Huh, K. Lee, Nanomaterials for Theranostics: recent advances and future challenges, Chem. Rev. 115 (2015) 327–394, https://doi.org/10.1021/cr300213b.
[12] J.E. Ferguson, R.A. Orlando, Curcumin reduces cytotoxicity of 5-fluorouracil treatment in human breast cancer cells, J. Med. Food 18 (2015) 497–502, https://doi.org/10.1089/jmf.2013.0086.
[13] A. Failli, R. Consolini, A. Legitimo, G. Orsini, A. Romanini, R. Spisni, M. Castagna, P. Miccoli, Evaluation of in vitro cytotoxicity of oxaliplatin and 5-fluorouracil in human colon cancer cell lines: combination versus sequential exposure, J. Biol. Regul. Homeost. Agents 25 (2011) 575–588.
[14] J.L. Arias, Novel strategies to improve the anticancer action of 5-fluorouracil by using drug delivery systems, Molecules 13 (2008) 2340–2369, https://doi.org/10.3390/molecules13102340.
[15] Q. Jin, F. Mitschang, S. Agarwal, Biocompatible drug delivery system for photo-triggered controlled release of 5-fluorouracil, Biomacromolecules 12 (2011) 3684–3691, https://doi.org/10.1021/bm2009125.
[16] A. Polk, K. Vistisen, M. Vaage-Nilsen, D.L. Nielsen, A systematic review of the pathophysiology of 5-fluorouracil-induced cardiotoxicity, BMC Pharmacol. Toxicol. 15 (2014)https://doi.org/10.1186/2050-6511-15-47.
[17] M. Novak, B. Zegura, B. Modic, E. Heath, M. Filipic, Cytotoxicity and genotoxicity of anticancer drug residues and their mixtures in experimental model with zebrafish liver cells, Sci. Total Environ. 601 (2017) 293–300, https://doi.org/10.1016/j.scitotenv.2017.05.115.
[18] R. Kovacs, Z. Csenki, K. Bakos, B. Urbanyi, A. Horvath, V. Garaj-Vrhovac, G. Gajski, M. Geric, N. Negreira, M. de Alda, D. Barcelo, E. Heath, T. Kosjek, B. Zegura, M. Novak, I. Zajc, S. Baebler, A. Rotter, Z. Ramsak, M. Filipic, Assessment of toxicity and genotoxicity of low doses of 5-fluorouracil in zebrafish (Danio rerio) two-generation study, Water Res. 77 (2015) 201–212, https://doi.org/10.1016/j.watres.2015.03.025.
[19] H. Luo, D. Ji, C. Li, Y. Zhu, G. Xiong, Y. Wan, Layered nanohydroxyapatite as a novel nanocarrier for controlled delivery of 5-fluorouracil, Int. J. Pharm. 513 (2016) 17–25, https://doi.org/10.1016/j.ijpharm.2016.09.004.
[20] G. Pan, T. Jia, Q. Huang, Y. Qiu, J. Xu, P. Yin, T. Liu, Mesoporous silica nanoparticles (MSNs)-based organic/inorganic hybrid nanocarriers loading 5-fluorouracil for the treatment of colon cancer with improved anticancer efficacy, Colloids Surfaces B Biointerfaces 159 (2017) 375–385, https://doi.org/10.1016/j.colsurfb.2017.08.013.
[21] S. Egodawatte, S. Dominguez, S.C. Larsen, Solvent effects in the development of a drug delivery system for 5-fluorouracil using magnetic mesoporous silica nanoparticles, Microporous Mesoporous Mater. 237 (2017) 108–116, https://doi.org/10.1016/j.micromeso.2016.09.024.
[22] K. Zhu, T. Ye, J. Liu, Z. Peng, S. Xu, J. Lei, H. Deng, B. Li, Nanogels fabricated by lysozyme and sodium carboxymethyl cellulose for 5-fluorouracil controlled release, Int. J. Pharm. 441 (2013) 721–727, https://doi.org/10.1016/j.ijpharm.2012.10.022.
[23] H.-C. Yang, M.-H. Hon, The effect of the molecular weight of chitosan nanoparticles and its application on drug delivery, Microchem. J. 92 (2009) 87–91, https://doi.org/10.1016/j.microc.2009.02.001.
[24] J.R. Lakkakula, T. Matshaya, R.W.M. Krause, Cationic cyclodextrin/alginate chitosan nanoflowers as 5-fluorouracil drug delivery system, Mater. Sci. Eng. C Mater. Biol. Appl. 70 (2017) 169–177, https://doi.org/10.1016/j.msec.2016.08.073.
[25] C. Ehi-Eromosele, B. Ita, E. Iweala, Silica coated LSMO magnetic nanoparticles for the pH-responsive delivery of 5-fluorouracil anticancer drug, Colloids Surfaces A Physicochem. Eng. Asp. 530 (2017)https://doi.org/10.1016/j.colsurfa.2017.07.059.
[26] E.A. Müller, K.E. Gubbins, Molecular simulation study of hydrophilic and hydrophobic behavior of activated carbon surfaces, Carbon N. Y. 36 (1998) 1433–1438, https://doi.org/10.1016/S0008-6223(98)00135-3.
[27] C. Moreno-Castilla, Adsorption of organic molecules from aqueous solutions on carbon materials, Carbon N. Y. 42 (2004) 83–94, https://doi.org/10.1016/j.carbon.2003.09.022.
[28] B. Singh, S. Lohan, P.S. Sandhu, A. Jain, S.K. Mehta, Chapter 15 - functionalized carbon nanotubes and their promising applications in therapeutics and diagnostics, in: A.M. Grumezescu (Ed.), Nanobiomaterials Med. Imaging, William Andrew Publishing 2016, pp. 455–478, https://doi.org/10.1016/B978-0-323-41736-5.00015-7.
[29] S. Merum, J.B. Veluru, R. Seeram, Functionalized carbon nanotubes in bio-world: applications, limitations and future directions, Mater. Sci. Eng. B 223 (2017) 43–63, https://doi.org/10.1016/j.mseb.2017.06.002.
[30] G. Tobias, E. Mendoza, B. Ballesteros, Functionalization of carbon nanotubes, in: B. Bhushan (Ed.), Encycl. Nanotechnol, Springer Netherlands, Dordrecht 2012, pp. 911–919, https://doi.org/10.1007/978-90-481-9751-4_48.
[31] M.K. Hazrati, N.L. Hadipour, Adsorption behavior of 5-fluorouracil on pristine, B-, Si-, and Al-doped C60 fullerenes: a first-principles study, Phys. Lett. A 380 (2016) 937–941, https://doi.org/10.1016/j.physleta.2016.01.020.
[32] G. Román, E. Noseda Grau, A. Díaz Compañy, G. Brizuela, A. Juan, S. Simonetti, A first-principles study of pristine and Al-doped activated carbon interacting with 5-fluorouracil anticancer drug, Eur. Phys. J. E. 41 (2018) 107, https://doi.org/10.1140/epje/i2018-11718-4.
[33] R. Bagheri, M. Babazadeh, E. Vessally, M. Es'haghi, A. Bekhradnia, Si-doped phagraphene as a drug carrier for adrucil anti-cancer drug: DFT studies, Inorg. Chem. Commun. 90 (2018) 8–14, https://doi.org/10.1016/j.inoche.2018.01.020.

[34] L.C. Qin, X.L. Zhao, K. Hirahara, Y. Miyamoto, Y. Ando, S. Iijima, Materials Science, The smallest carbon nanotube, Nature 408 (2000) 50, https://doi.org/10.1038/35040699.
[35] M.J. Frisch, G.W. Trucks, H.B. Schlegel, G.E. Scuseria, M.A. Robb, J.R. Cheeseman, G. Scalmani, V. Barone, B. Mennucci, G.A. Petersson, H. Nakatsuji, M. Caricato, X. Li, H.P. Hratchian, A.F. Izmaylov, J. Bloino, G. Zheng, J.L. Sonnenberg, M. Hada, M. Ehara, K. Toyota, R. Fukuda, J. Hasegawa, M. Ishida, T. Nakajima, Y. Honda, O. Kitao, H. Nakai, T. Vreven, J.A. Montgomery, J.E. Peralta, F. Ogliaro, M. Bearpark, J.J. Heyd, E. Brothers, K.N. Kudin, V.N. Staroverov, R. Kobayashi, J. Normand, K. Raghavachari, A. Rendell, J.C. Burant, S.S. Iyengar, J. Tomasi, M. Cossi, N. Rega, J.M. Millam, M. Klene, J.E. Knox, J.B. Cross, V. Bakken, C. Adamo, J. Jaramillo, R. Gomperts, R.E. Stratmann, O. Yazyev, A.J. Austin, R. Cammi, C. Pomelli, J.W. Ochterski, R.L. Martin, K. Morokuma, V.G. Zakrzewski, G.A. Voth, P. Salvador, J.J. Dannenberg, S. Dapprich, A.D. Daniels, Farkas, J.B. Foresman, J.V. Ortiz, J. Cioslowski, D.J. Fox, Gaussian 09, Revision E.01, Gaussian Inc, Wallingford CT, 2009.
[36] A.D. Becke, A new mixing of hatree-fock and local density functional theories, J. Chem. Phys. 98 (1993) 1372–1377, https://doi.org/10.1063/1.464304.
[37] Y. Zhao, C. Huang, M. Kim, B.M. Wong, F. Léonard, P. Gopalan, M.A. Eriksson, Functionalization of single-wall carbon nanotubes with chromophores of opposite internal dipole orientation, ACS Appl. Mater. Interfaces 5 (2013) 9355–9361, https://doi.org/10.1021/am4024753.
[38] C. Huang, R.K. Wang, B.M. Wong, D.J. McGee, F. Léonard, Y.J. Kim, K.F. Johnson, M.S. Arnold, M.A. Eriksson, P. Gopalan, Spectroscopic properties of nanotube–chromophore hybrids, ACS Nano 5 (2011) 7767–7774, https://doi.org/10.1021/nn202725g.
[39] C. Tabtimsai, S. Keawwangchai, N. Nunthaboot, V. Ruangpornvisuti, B. Wanno, Density functional investigation of hydrogen gas adsorption on Fe-doped pristine and stone-Wales defected single-walled carbon nanotubes, J. Mol. Model. 18 (2012) 3941–3949, https://doi.org/10.1007/s00894-012-1388-1.
[40] H.H. Bouzari, L.F. Matin, R. Malekfar, A. Shafiekhani, Experimental and theoretical investigation of spontaneous and surface-enhanced Raman scattering (SERS) spectroscopy of pure and boron-doped carbon nanotubes, J. Theor. Appl. Phys. 12 (2018) 101–111, https://doi.org/10.1007/s40094-018-0286-z.
[41] M. Yoosefian, M. Zahedi, A. Mola, S. Naserian, A DFT comparative study of single and double SO2 adsorption on Pt-doped and Au-doped single-walled carbon nanotube, Appl. Surf. Sci. 349 (2015) 864–869, https://doi.org/10.1016/j.apsusc.2015.05.088.
[42] M. Yoosefian, N. Etminan, Pd-doped single-walled carbon nanotube as a nanobiosensor for histidine amino acid, a DFT study, RSC Adv. 5 (2015) 31172–31178, https://doi.org/10.1039/c5ra00834d.
[43] S.F. Boys, F. Bernardi, The calculation of small molecular interactions by the differences of separate total energies. Some procedures with reduced errors, Mol. Phys. 19 (1970) 553–566, https://doi.org/10.1080/00268977000101561.
[44] R. Jawaria, M. Hussain, M. Khalid, M.U. Khan, M.N. Tahir, M.M. Naseer, A.A. Carmo Braga, Z. Shafiq, Synthesis, crystal structure analysis, spectral characterization and nonlinear optical exploration of potent thiosemicarbazones based compounds: a DFT refine experimental study, Inorganica Chim. Acta. 486 (2019) 162–171, https://doi.org/10.1016/j.ica.2018.10.035.
[45] R.G. Parr, R.G. Pearson, Absolute hardness - companion parameter to absolute electronegativity, J. Am. Chem. Soc. 105 (1983) 7512–7516, https://doi.org/10.1021/ja00364a005.
[46] P. Geerlings, F. De Proft, W. Langenaeker, Conceptual density functional theory, Chem. Rev. 103 (2003) 1793–1873, https://doi.org/10.1021/cr990029p.
[47] N.M. O'Boyle, A.L. Tenderholt, K.M. Langner, Cclib: a library for package-independent computational chemistry algorithms, J. Comput. Chem. 29 (2008) 839–845, https://doi.org/10.1002/jcc.20823.
[48] T. Lu, F. Chen, Multiwfn: a multifunctional wavefunction analyzer, J. Comput. Chem. 33 (2012) 580–592, https://doi.org/10.1002/jcc.22885.
[49] R. Dennington, T.A. Keith, J.M. Millam, GaussView 5.0.9, 2009.
[50] W. Humphrey, A. Dalke, K. Schulten, VMD: Visual molecular dynamics, J. Mol. Graph. 14 (1996) 33–38, https://doi.org/10.1016/0263-7855(96)00018-5.
[51] T. Yanai, D.P. Tew, N.C. Handy, A new hybrid exchange–correlation functional using the Coulomb-attenuating method (CAM-B3LYP), Chem. Phys. Lett. 393 (2004) 51–57, https://doi.org/10.1016/j.cplett.2004.06.011.
[52] İ. Muz, M. Kurban, Enhancement of electronic, photophysical and optical properties of 5,5′-Dibromo-2,2′-bithiophene molecule: new aspect to molecular design, Opto-Electronics Rev 27 (2019) 113–118, https://doi.org/10.1016/j.opelre.2019.03.002.
[53] M. Kurban, B. Gündüz, F. Göktaş, Experimental and theoretical studies of the structural, electronic and optical properties of BCzVB organic material, Optik (Stuttg) 182 (2019) 611–617, https://doi.org/10.1016/j.ijleo.2019.01.080.
[54] E. Shakerzadeh, Quantum chemical assessment of the adsorption behavior of fluorouracil as an anticancer drug on the B 36 nanosheet, J. Mol. Liq. 240 (2017) 682–693, https://doi.org/10.1016/j.molliq.2017.05.128.
[55] Z. Khalili, M.D. Ganji, M. Mehdizadeh, Fluorouracil functionalized Pt-doped carbon nanotube as drug delivery nanocarrier for anticarcinogenic drug: a B3LYP-D3 study, J. Nanoanalysis. 5 (2018) 202–209, https://doi.org/10.22034/jna.2018.542770.
[56] Ö. Alver, C. Parlak, P. Ramasami, M. Şenyel, Interaction between doped C60 fullerenes and piperazine-2,3,5,6-tetraone: DFT simulation, Main Gr. Met. Chem. 41 (2018) 63–66, https://doi.org/10.1515/mgmc-2017-0054.
[57] Y. Gökpek, M. Bilge, D. Bilge, Ö. Alver, C. Parlak, Adsorption mechanism, structural and electronic properties: 4-Phenylpyridine & undoped or doped (B or Si) C60, J. Mol. Liq. 238 (2017) 225–228, https://doi.org/10.1016/j.molliq.2017.04.128.
[58] F. Hassani, H. Tavakol, A DFT, AIM and NBO study of adsorption and chemical sensing of iodine by S-doped fullerenes, Sensors Actuators B Chem. 196 (2014) 624–630, https://doi.org/10.1016/j.snb.2014.02.051.
[59] I. Mayer, P. Salvador, Overlap populations, bond orders and valences for `fuzzy' atoms, Chem. Phys. Lett. 383 (2004) 368–375, https://doi.org/10.1016/j.cplett.2003.11.048.
[60] T. Lu, F. Chen, Bond order analysis based on the laplacian of electron density in fuzzy overlap space, J. Phys. Chem. A 117 (2013) 3100–3108, https://doi.org/10.1021/jp4010345.
[61] C. Parlak, Ö. Alver, A density functional theory investigation on amantadine drug interaction with pristine and B, Al, Si, Ga, Ge doped C60 fullerenes, Chem. Phys. Lett. 678 (2017) 85–90, https://doi.org/10.1016/j.cplett.2017.04.025.
[62] E.R. Johnson, S. Keinan, P. Mori-Sánchez, J. Contreras-García, A.J. Cohen, W. Yang, Revealing noncovalent interactions, J. Am. Chem. Soc. 132 (2010) 6498–6506, https://doi.org/10.1021/ja100936w.